Spreading of a lidocaine formulation on microneedle treated skin

Atul Nayak, Diganta B. Das*, Tzu C. Chao, Victor M. Starov

Department of Chemical Engineering, Loughborough University, Loughborough LE11 3TU, Leicestershire, UK

*Corresponding author (Email: D.B.Das@lboro.ac.uk)

Abstract

The spreadability of a liquid drug formulation on skin is an indication of it either remaining stationary or distributing (spreading) as a droplet. Factors determining droplet spreadability of the formulation are spreading area, diameter of the droplet base, viscosity of the liquid, contact angle, volume of droplet on skin and any others. The creation of microcavities from the application of microneedle (MN) has the potential to control droplet spreading, and hence, target specific areas of skin for drug delivery. However, there is little work that demonstrates spreading of liquid drug formulation on MN treated skin. Below, spreading of a lidocaine hydrogel formulation and lidocaine solution (reference liquid) on porcine skin is investigated over MN treated skin. Controlled spreadability was achieved with the lidocaine hydrogel on MN treated skin as compared with lidocaine solution. It was observed that the droplet spreading parameters such as spreading radius, droplet height and dynamic contact angle were slightly lower for the lidocaine hydrogel than the lidocaine solution on skin. Also, the lidocaine hydrogel on MN treated skin resulted in slower dynamic reduction of droplet height, contact angle and reduced time taken in attaining static advancing droplets due to the MN microcavities.

Keywords: Spreadability; Lidocaine; Microneedles; Microcavities; Porcine Skin

1.0 Introduction

Percutaneous absorption/permeation of a drug molecule (e.g., lidocaine) through skin depends on the contact between the formulation and skin properties through which the drug molecules are absorbed into different skin layers. The possibility of the drop of a liquid drug formulation either remaining static or distributing (spreading) horizontally on the skin surface relies on its spreadability. If the droplet is capable of spreading, then the contact line between the formulation and skin moves over the skin. The rate of movement of the contact line can be defined as the spreadability of the formulation.

Spreadability has significant importance in localised application and efficacy of topical drugs (Chow et al., 2007). However, the characteristic time scales for spreading of a drug formulation on skin (~seconds to minutes) is significantly smaller than the characteristic time scales for drug absorption/permeation into skin (~10s of minutes to hours). Therefore, most studies of percutaneous or transdermal drug delivery do not characterise spreading behaviour of the drug formulation over skin. Spreadability is primarily determined by the area/diameter of the

formulation droplet on a substrate (e.g., skin below), viscosity of the formulation, contact angle, the volume of a droplet (permeant amount) (Jelvehgari and Montazam, 2011), and other factors.

Over recent years a number of researchers have discussed the possibility of enhanced permeation of lidocaine (a common anaesthetic) via a 'poke and patch' approach with the help of solid microneedle (MN) arrays (Banks et al., 2011; Hamzah et al., 2012; Nayak et al., 2014a,b). This approach involves treating the skin with well-defined MNs to create microcavities in skin followed by the deposition of a droplet of lidocaine solution on the MN treated area. For example, Nayak et al. (2014a,b, 2015) demonstrated this approach using a lidocaine NaCMC:gel 1:2.3 hydrogel formulation and determined the permeation profiles of lidocaine in porcine skin. While the lidocaine droplets spread over the skin, the lidocaine molecules also permeate through the treated area (Nayak et al., 2014a,b; Nayak et al., 2015). The duration of lidocaine hydrogel droplet spreading is in seconds, which is much faster as compared with that for drug permeation which normally takes about an hour to reach equilibrium lidocaine concentration in skin.

It is known that MNs have been primarily developed to control the mass transfer distance and time as a drug molecule is absorbed in the skin. However, the creation of microcavities using MN to accelerate penetration in the skin (Figure 1) allows controlling of spreading of the drug formulation droplet on skin and, hence, targeting a specific skin area over which the drug absorption/permeation can take place. On the other hand, a liquid droplet on a normal skin (i.e., untreated skin) is likely to spread in a low controlled manner, with low reproducibility and more rapidly as compared with a MN treated skin. At the moment, there is little or no study that specifically analyses in detail such spreading dynamics of drug formulation on MN pierced skin and the role that the MN cavities play in determining the formulation spreading behaviour. This work aims to address this gap.

Below, lidocaine was loaded in a hydrogel biopolymer with a gel to NaCMC mass ratio of 2.3 as discussed earlier in Nayak et al. (2014a,b) and Nayak et al. (2015). This mass ratio represents optimum drug and vehicle physico-chemical properties for a formulation (Nayak et al., 2014a,b). For the developed approach, controlling the spreadability of lidocaine hydrogel on skin is important to acquire liquid distribution of a liquid over the skin surface. A slower droplet spreading on skin coupled with a faster time in attaining static advancing contact angle is a favourable outcome in ensuring localised permeation of lidocaine at the treatment site.

Lidocaine NaCMC:gel 1:2.3 hydrogel is a non-Newtonian liquid at standard room temperatures and pressure (Nayak et al., 2014a). The Ostwald de Waele power law can be used to describe the pseudoplastic behaviour of for such a fluid as follows:

$$\eta = k(\gamma)^{n-1} \quad . \tag{1}$$

Where η is the apparent viscosity, γ is the shear rate, k is the consistency constant of the substance and n is the power-law or flow index. A log-log plot of viscosity (η) on shear rate (γ)

for lidocaine NaCMC:gel 1:2.3 taken from Nayak et al. (2014a) provides an index value n = 0.392. As the index value is less than 1, the fluid is identified as pseudoplastic (Fang and Hanna, 1999). Its physical property can be exploited in quantifying and controlling the spreading of a lidocaine hydrogel droplet on an untreated flat skin surface without the need for manual rubbing across the whole area. For example, the pseudoplastic properties of the hydrogel is likely to provide a better control in droplet spreading as discussed earlier by Nayak et al. (2014b).

Below a comparison of spreadability between lidocaine NaCMC:gel 1:2.3 hydrogel (higher viscosity) and lidocaine solution (lower viscosity) is conducted in order to understand the spreading behaviour. The loading dosage of lidocaine in both the hydrogel and solution form containing water was 2.4% w/w. The objective of the study is to examine the spreadability of lidocaine NaCMC:gel 1:2.3 hydrogel droplets on MN treated and untreated skin in relation to the viscosity of the formulation. Surface layers of skin treated with MN contain microcavities, which allow controlling the spreading of the lidocaine hydrogel and achieving static advancing contact angles and decreased spreading radius faster as compared with untreated skin. Three different MN types are applied to the skin samples in order to create controlled cavity depths past ~ 15μm thick stratum corneum (SC) layer of skin. Evaporation of the droplet is defined to be negligible due to the high boiling point of residual paraffin content in the lidocaine hydrogel, and relatively short duration of the spreading experiments. Our study specifically focuses on a drug formulation spreading on MN treated skin, which is the first attempt to investigate this process to the best of our knowledge.

2.0 Materials and Methods

A lidocaine NaCMC:gel 1:2.3 hydrogel formulated by Nayak et al. (2014a) was adopted for characterising spreadability on porcine skin. The method of preparation of the hydrogel can be found in Nayak et al. (2014a,b) and Nayak et al. (2015). As stated earlier, the gel to NaCMC mass ratio of 2.3 was chosen for this study because of a faster permeation of lidocaine into the skin. The lidocaine NaCMC:gel 1:2.3 hydrogels were formulated using the vacuum oven method during final stage evaporation of excess paraffin dissolved in n-hexane as described in Nayak et al. (2014a,b). To prepare lidocaine solution, lidocaine HCl (> 98% assay) was added to deionised water and heated gently to ensure a dissolved solution at 2.4% w/w. However, no lidocaine permeability experiments were conducted below. This work is focussed on determining the spreading radii, droplet heights, dynamic contact angles and characteristic spreading times of lidocaine hydrogel and solution (i.e., lidocaine dissolved in deionised water) on both porcine skin and an artificial skin membrane, namely, Strat-M.

2.1 Reagents and Materials

Lidocaine HCl (Sigma Aldrich UK, Dorset, UK), lidocaine NaCMC:gel 1:2.3 hydrogels, autopipette 0-10 μl (Thermofisher Ltd, Warrington, UK), Camera i-speed LT high speed video (Olympus, Essex, UK), MNs (AdminPatch, California, U.S.A), porcine skin (local butcher, UK), piston enabled pressure/force device (SMC pneumatics Ltd, Buckinghamshire, UK), synthetic transdermal membrane (Strat-M™, Merck Millipore, Hertfordshire, UK), temperature and

humidity probe (Standard, Maplin Electronics, Leicestershire, UK) were used in experiments below.

2.2 Preparation of skin for spreading experiments

The procedures for skin preparation were similar to the ones used for Franz diffusion cell (FDC) experiments for determining drug permeation in skin, e.g., please see methods stated by Nayak et al. (2014a,b). Briefly, these procedures involved the following steps: (i) either fresh porcine skin pieces originating from the porcine ears were washed in deionised water and dried using a tissue, or frozen porcine skin pieces originating from the porcine ears were thawed at room temperature, washed in deionised water and dried using a tissue; (ii) the cartilage, subcutaneous fat, blood vessels and connective tissue were removed from the underlying dermis sections of all skin samples; (iii) the skin samples were dissected further into 10 mm x 10 mm square pieces; (iv) the skin was placed on microscope slides with SC layer facing upwards for observation of the spreading dynamics.

2.3 MN treatment of skin

Stainless steel MNs of two lengths (1100μm and 600μm) were placed in the centre of a prepared porcine skin sample. A perpendicular piston barrel device (SMC pneumatics Ltd, serial: CD85N16-50-B) was used for transmission of controlled pressure induced force onto the chosen MN as described by Cheung et al. (2014). Using the system, constant pressures of 0.5 bar, 1.0 bar and 2.0 bar equating to impact forces of 3.9 N, 7.9 N and 15.7 N were held for five minutes on the base of the MN (Nayak et al., 2015; Cheung et al., 2014). The forces (3.9 N, 7.9 N and 15.7 N) used to treat the skin with the MNs (Nayak et al., 2015). The MN patch was removed from the porcine skin prior to droplet spreading experiments.

2.4 Spreading of lidocaine NaCMC:gel 1:2.3 over skin surface

The experimental procedures for studying the spreading of lidocaine hydrogel droplet on porcine skin were adapted from Chao et al. (2014). A lidocaine hydrogel droplet (volume of 3.0 ± 0.5 μl) was deposited using a pipet onto a piece of skin resting on a microscope slide as carefully as possible to prevent splashing or fast inertial spreading. The i-speed LT high speed camera (Olympus, UK) recorded 1.85 frames per second until a stationery droplet profile or full disappearance was reached. The procedure was repeated twice for the control lidocaine solution. The real time capture of stages of the droplet spreading by camera configurations (i-speed, LT high speed) focused on the droplet is presented in Figure 2. This arrangement is based on liquid spreading and imbibition experiments for Newtonian liquids (Chao et al., 2014)

2.5 Spreading of lidocaine NaCMC:gel 1:2.3 hydrogels on the surface of artificial skin Strat-M membrane

Besides porcine skin, synthetic membrane which is sometimes used as a substitute for skin in transdermal *in vitro* studies were used as a substrate. These are composed of polyethersulfone and polyolefin and are known by the trade name Strat-M (Merck Millipore Ltd, Hertfordshire, UK). Strat-M membranes were chosen as control matrices for spreadability studies because of a relatively uniform flat surface as compared with the less uniform and rough surfaces of natural skin samples.

The characterisation of droplet spreading parameters, especially contact angles, was adopted from Chao et al. (2014). A square section of membrane substrate (15 mm x 15 mm) from a larger section was cut and taped to an edge of the glass side. This allows closer distance and improved resolution between the droplet and the camera lens. A hydrogel droplet of volume 3.0 ± 0.5 µl was immediately deposited on the membrane in the same way as in the case a natural skin. The recording procedure was identical to that described in the previous section. The droplet images of all formulations used were processed using Vision Builder software (National Instrument, UK) to determine droplet spreading parameters: contact angle, droplet height and spreading radius.

2.6 The measurement of relative humidity and temperature

The percentage relative humidity (% RH) and temperature of the droplet environment were recorded using an electronic probe (Standard, Maplin Electronics, Leicestershire, UK). The data were acquired in triplicate.

3.0 Results and Discussion

Comparative trends for lidocaine droplet spreading on porcine skin samples and Strat-M membrane were deduced starting with lidocaine solution as a control sample. The results are discussed below.

3.1 Spreadability of lidocaine 2.4 % w/w solution (lidocaine dissolved in DI water)

The spreading of lidocaine 2.4% w/w solution droplets on normal skin (i.e., untreated porcine skin) were significantly more rapid and showed an almost linear dependence of spreading radius on time as compared with those for MN treated skin (Figure 3a). Likewise, the droplet heights of lidocaine solution droplets showed faster reduction and the droplet heights at static profiles was achieved after approximately 130 seconds (Figure 4a). The dynamic contact angle for the same case showed a faster reduction reaching the static advancing contact angle approximately of 11˚ after 130 seconds (Figure 5a). A sharp reduction in the contact angle was observed within the first 40 seconds for the lidocaine solution on the untreated skin. This suggests a slightly steeper reduction profile as compared with that for the lidocaine solution on 3.9 N MN treated skin for MNs of 600 and 1100µm lengths, respectively (Figure 5d). The microcavity depths for both 600µm and 1100µm long MNs are expected to be shallow for the force applied on the MNs (Nayak, et al., 2015) and, therefore, significantly less reduction in the contact angles was observed when compared with those for non-MN treated skin (Figure 5c).

Droplets of the lidocaine solution have an initial contact angle of 57.1° at the moment of deposition ($t \cong 0$) on the non-MN treated skin. The viscosity of lidocaine solution is very similar to DI water and both are Newtonian fluids. However, the initial contact angle was near 90° for DI water on non-MN treated skin as reported earlier by Elkhyat et al. (2004), which is significantly higher than observed for the lidocaine solution. The high contact angle of DI water was caused

by the low sebum content on skin and there is a big variation in the initial contact angle depending on skin location (Elkhyat et al., 2004). Sebum is a natural mixture of lipids. Lidocaine solution on non-MN treated skin is devoid of artificial cavities and excess liquid cannot retain inside cavities and slow down droplet spreading.

The 1100 μm long MN induced microcavity depths for 3.9 N, 7.9 N and 15.7 N forces are reported to be 19.5 μm, 23.1 μm and 26.7 μm, respectively (Nayak et al., 2015). The mean microcavity depths using 600 μm long MN for the same forces are small but they are not easily detectable for transverse visualisation of skin microcavities as the forces applied are relatively small (implying smaller microcavity length). However, AdminPatch™ microneedles at 600μm length are shown to increase drug permeation. For example, drug permeability studies by Kaur et al. (2014) demonstrated a 14.3 fold increase in permeation flux as compared with passive diffusion for the transdermal delivery of an anti-hypertensive agent, thus implying that microcavities were formed in skin. These depths cross the typical SC layer depth of 15 μm (Nayak et al., 2015).

The dynamic contact angles of lidocaine solution on 7.9 N force treated MN skin outlines slow decreases in contact angles, which is especially more significant for the 1100 μm long MNs (Figure 5a). The spreading radius and droplet height of lidocaine solution are significantly less for 7.9 N force treated skin (Figures 3a and 4a). This is because of deeper MN cavities capturing excess liquid during droplet spreading of lidocaine solution. Nevertheless, it was not possible to determine using conventional cryotome techniques if a large quantity of MN in a patch created a uniform depth microcavity for both specific MN lengths. MNs were impacted on skin for 5 minutes maximum using one specific force, so an assumption that most MNs have successfully pierced skin at significant microcavity depths will be made here.

3.2 Spreadability of lidocaine NaCMC:gel 1:2.3 hydrogel

The spreading of lidocaine NaCMC:gel 1:2.3 hydrogel show similar trends for 600μm long MN treated skin, particularly closer for 3.8 N and 7.8 N forces (Figure 3c). The fluid properties of the formulation which affect the spreading behaviour have been discussed earlier (Nayak et al., 2014a, b).

The 15.7 N force on a 600μm MN patch treated skin showed increasing spreading radius than 3.9 N as compared with the lowest force of the same MN length (Figure 3c). This is because the MN cavity depths are likely not to be deep enough. The reason is because of an observable reduction in spreading radius caused by deeper micro-cavities from higher MN forces. Lidocaine hydrogel droplets for the insertion forces of 3.9 N, 7.9 N and 15.7 N for 1100 μm long MNs provide less rapidly increasing spreading radius, less rapidly decreasing droplet heights and less rapidly decreasing dynamic contact angles (Figures 3c, 4c and 5c) before static profiles were reached. Nevertheless, there were minor contradictions in reporting lower spreading radii when droplet heights were not decreasing rapidly because of the mild pseudoplastic properties of the lidocaine hydrogel (Nayak et al., 2014a). For example, lidocaine hydrogel from 3.9 N, 600μm treated skin should hypothetically outline faster spreading than 7.9 N, 1100μm on skin because the latter usually possess deep microcavites (Figure 3c). Skin microcavities created by

MNs do not produce exact replicates of microcavity lengths as shown in transverse section micrographs due to variability in the viscoelastic property of skin (Nayak et al., 2015). Further, lidocaine hydrogel droplets were sometimes difficult to dispense with accurate volumes within ± 0.05 µl because of the viscous nature of the formulation.

The results show that the lidocaine solution spreading radii for 3.9 N and 7.9 N forces of 1100 µm long (longer MNs) MN is distinctly different as compared to the lidocaine hydrogel spreading radii (Figures 3a and 3c). However, no significant difference in droplet spreading radii was observed when comparing 3.9 and 7.9 N force of 600 µm long MN (shorter MNs) for lidocaine solution (Figure 3a). In further scrutinising spreading patterns the lidocaine solution showed rapid spreading, faster decrease in droplet height and rapid decrease in dynamic contact angle as compared with lidocaine hydrogel when the same forces, namely, 3.9 N force was applied on the skin (Figure 3d).

The artificial membrane (Strat-M), which is normally implemented in drug based *in vitro* passive diffusion studies, was a control for skin because of a relatively smooth surface (Uchida et al., 2015). The spreading radii of lidocaine solution and hydrogel droplets could not be measured reliably with a good repeatability because of the horizontal placement of camera and liquid percolation through the pores in the membrane. However, there is a slight decrease in droplet height and dynamic contact angle for lidocaine solution droplets (Figures 4b and 5b). This slight decrease can be attributed to the percolation of lidocaine solution into Strat-M pores despite no significant change in droplet spreading radius.

Lidocaine hydrogel droplets showed significant change in spreading radius, droplet height and dynamic contact angle (Figures 4b, 5b) on Strat-M. The droplet spreading was likely to be caused by the lower surface tension of lidocaine hydrogel on the hydrophobic surface of Strat-M. Lidocaine hydrogel contains residual paraffin of low surface tension properties as compared with water.

Lidocaine hydrogels and lidocaine solution droplets snapshots outline spreading in terms of observed changes in droplet shape at three distinct timings (Figures 6 and 7). Lidocaine solution droplets have dome shape at the initial time of placement as compared with slightly flattened dome shaped droplets for lidocaine hydrogel (Figures 6 and 7). After a duration of 10 seconds, the lidocaine hydrogels spread more than the lidocaine solution, especially on skin treated with 600 µm long MNs (Figures 6 and 7). In most cases, lidocaine solution shows distinct droplet with respect to 7.9 N force with 1100µm long MN treated skin and Strat-M membrane after 180 seconds (Figure 6). The remaining MN treated skin variables appear not to retain more lidocaine solution droplets in the microcavities (Figure 6). After the duration of 180 seconds, the droplet outline is distinctly notable for lidocaine hydrogel after 1100µm MN treatment on skin (Figure 7).

The relative humidity and temperature of the surrounding vicinity for droplet spreadability was 48.6±4.31% at 20.1˚±2.40˚C, respectively. The standard deviation for relative humidity is observed because the surroundings are not an isolated system preventing the transfer of heat.

Normal environmental changes in relative humidity were expected because the duration of experiments were conducted upto 3 minutes and relative humidity can fluctuate in a matter of seconds. The reading of relative humidity of 48.6% is near average at a low room temperature. The likelihood of evaporation is low for these surrounding conditions and the short duration of the experiments.

3.3 Dimensionless spreading parameters of lidocaine hydrogel and solution

The spreading dynamics of lidocaine NaCMC:gel 1:2.3 hydrogel and solution are represented in this section in terms of dimensionless parameters, namely, dimensionless spreading radius ($\frac{L_t}{L_m}$), dimensionless contact angle ($\frac{\theta_t}{\theta_m}$), dimensionless droplet height ($\frac{h_t}{h_m}$) and dimensionless spreading time ($\frac{t}{t^*}$) and dimensionless droplet volume $\left(\frac{V_t}{V_{max}}\right)$. For the above five dimensionless parameters, the numerators, namely, L_t, θ_t, h_t, V_t and t, are the droplet spreading radius, contact angle, height, volume and measured time periodically at different time intervals. On the other hand, the denominators of the fractions are the droplet base showing the maximum spreading radius, maximum contact angle, maximum droplet height, maximum droplet volume and static advancing droplet time. The dimensionless numbers, namely, $\frac{L_t}{L_m}$, $\frac{\theta_t}{\theta_m}$, $\frac{h_t}{h_m}$ and $\frac{V_t}{V_{max}}$ are plotted as function of $\frac{t}{t^*}$ for various circumstances (Figure 8). Analyses of these parameters provide understanding of the time evolution of these parameters and give some generality to the results (e.g., see Chao et al., 2014). Figure 8 shows that the time evolutions of these dimensionless parameters are different implying that the spreading behaviour is different in different cases. These are discussed below.

The lidocaine hydrogel spreading on 3.9 N and 7.9 N force treated skin with 1100μm and 600 μm long MN showed short durations in increasing dimensionless spreading profiles, thus attaining closeness to a plateau of dimensionless value of 1.0 at a shorter time interval (Figure 8a). The lidocaine solution on non-MN treated skin could not be reported as dimensionless spreading because a linear profile was observed and L_m could not be deduced because of no plateau (Figure 3a).

The spreading of lidocaine hydrogels on 7.9 N and 15.7 N force treated skin with 1100 μm long MN showed a long durations in increasing spreading radius; thus, attaining closeness to dimensionless value 1.0 above the fractional time of 0.90 (Figure 8a). A short duration in increasing dimensionless spreading means a less dynamic spreading across the skin. As mentioned earlier in this paper, the lidocaine hydrogel fill the skin microcavities and the spreading of the hydrogel slow down.

All lidocaine hydrogels droplets on MN treated skin outlined slower reduction of dimensionless droplet height as the liquid fills the microcavities on MN treated skin (Figure 8b). Comparatively, the lidocaine solutions showed faster dynamic height reduction from maximum spreading height (t = 0) because of high initial droplet height fractions and faster spreading (Figure 8b).

Slower dynamic reduction of contact angle was observed for all lidocaine hydrogel droplets on MN treated skin (Figure 8c). The lidocaine hydrogel on 3.9 N of 1100 μm length, 7.9 N and 15.7 N of 600 μm treated skin showed slightly slower reductions in fractional contact angles (Figure 8c). Nevertheless, lidocaine hydrogel on 7.9 N and 15.7 N treated skin samples with 1100 μm long MN outlined slightly faster reductions in the dimensionless contact angle (Figure 8c). Static advancing droplets were found to arrive at shorter fractional timings for lidocaine hydrogels because of the viscous property of the hydrogel and presence of numerous MN microcavities as liquid percolates into the microcavity spaces.

The lidocaine solution droplets show significantly more dynamic volume decreases as compared with lidocaine hydrogel droplets (Figure 9 a,b), which is due to the fact that the lidocaine solution percolates into the MN holes faster than the lidocaine hydrogel droplets. The lidocaine hydrogels outline low droplet volume reductions in microneedle treated skin and fast appearance of static droplet volumes (Figure 9b). There was a faster reduction in droplet volume for Strat-M and 15.7 N, 1100 μm treated skin (Figure 9b). The roughness of skin and the pseudoplastic properties of the hydrogel are two factors in explaining the likelihood for the observed static advancing droplet profiles. Non-microneedle treated skin and Strat-M membrane surfaces appear smooth, so there appears to be faster droplet volume decreases in those two substrate control parameters.

4.0 Conclusion

The spreading of a liquid drug formulation, namely, lidocaine NaCMC:gel 1:2.3 hydrogel, on MN treated skin is studied. The results of the study show improved control of the formulation spreadability as compared to those for lidocaine solution (lidocaine dissolved in deionised water) alone. Lidocaine NaCMC:gel 1:2.3 hydrogel show a slightly lower spreading radius, sight decrease in droplet height and smaller, controlled decrease in dynamic contact angle as compared with lidocaine solution. The slower dynamic reduction of droplet height and contact angle and convergence to static advancing droplet at short initial timings for lidocaine NaCMC:gel 1:2.3 hydrogel are indication of the seepage of the liquid inside MN microcavities in skin.

5.0 References

Banks SL, Paudel KS, Brogden NK, Loftin CD, Stinchcomb AL (2011) Diclofenac enables prolonged delivery of naltrexone through microneedle-treated skin 28: 1211-1219

Butt HJ, Golovko DS, Bonaccurso E (2007) On the derivation of Young's equation for sessile Drops: nonequilibrium effects due to evaporation. J Phys Chem B 111: 5277-5283.

Chao TC, Trybala A, Starov V, Das DB (2014) Influence of haematocrit level on the kinetics of blood spreading on thin porous medium during dried blood spot sampling. Colloids and Surfaces A: Physicochemical and Engineering Aspects 451: 38-47.

Cheung K, Han T, Das DB (2014) Effect of force of microneedle insertion on the permeability of insulin in skin. Journal of Diabetes Science and Technology 8: 444-452.

Chow KT, Chan LW, Heng PWS (2008) Characterization of spreadability of nonaqueous ethylcellulose gel matrices using dynamic contact angle. Journal of Pharmaceutical Sciences 97: 3467-3481.

Courbin L, Bird JC, Reyssat M, Stone HA (2009) Dynamics of wetting: from inertial spreading to viscous imbibition. Journal of physics: Condensed matter 21: 1-13.

Elkhyat A, Courderot-Masuyer C, Mac-Mary S, Courau S, Gharbi T, Humbert P (2004) Assessment of spray application of Saint GERVAIS® water effects on skin wettability by contact angle measurement comparison with bidistilled water. Skin Research and Technology 10: 283-286.

Fang Q, Hanna MA (1999) Rheological properties of amorphous and semicrystalline polylactic acid polymers. Industrial Crops and Products 10: 47-53.

Hamzah AA, Aziz NA, Majlis BY, Yunas J, Dee CF, Bais B (2012) Optimization of HNA etching parameters to produce high aspect ratio solid silicon microneedles. Journal of Micromechanics and Microengineering 22: 1-10.

Jelvehgari M, Montazam H (2011) Evaluation of mechanical and rheological properties of metronidazole gel as local delivery system. Archives of Pharmacal Research 34: 931-940.

Kaur M, Ita KB, Popova IE, Parikh SJ, Bair DA (2014) Microneedle-assisted delivery of verapamil hydrochloride and amlodipine besylate. European Journal of Pharmaceutics and Biopharmaceutics 86: 284-291.

Nayak A, Das DB, Vladisavljević GT (2014a) Microneedle-assisted permeation of lidocaine carboxymethylcellulose with gelatine co-polymer hydrogel. Pharmaceutical Research 31:1170–1184

Nayak A, Babla H, Tao H, Das DB (2014b) Lidocaine carboxymethylcellulose with gelatine co-polymer hydrogel delivery by combined microneedle and ultrasound. Drug Delivery. (Article in press) DOI: 10.3109/10717544.2014.935985

Nayak A, Short L, Das DB (2015) Lidocaine permeation from a lidocaine NaCMC/gel microgel formulation in microneedle pierced skin: vertical (depth averaged) and horizontal permeation profiles. Drug Delivery and Translational Research. (Article in press). DOI: 10.1007/s13346-015-0229-z

Shields PA, Ling TF, Tjatha V, Shah DO, Farraha SR (1986) Comparison of positively charged membrane filters and their use in concentrating bacteriophages in water. Water Research 20: 145-151.

Strat-M. Compound Correlation Tool. Lidocaine (Analgesic) http://fa24f31db0da67276cd1-be593b508d6f5ef1fdddadaa02b1fbea.r66.cf1.rackcdn.com/stratm2.html (Accessed: 08/04/2015).

Tarleton ES, Wakeman RJ (1994) Understanding flux decline in crossflow microfiltration: Part 3. Effects of membrane morphology. Trans IChemE 72 (A): 521-529.

Uchida T, Kadhum WR, Kanai S, Todo H, Oshizaka T, Sugibayashi K (2015) Prediction of skin permeation by chemical compounds using the artificial membrane, Strat-M™. European Journal of Pharmaceutical Sciences 67: 113-118

Ukiwe C, Kwok DY (2005) On the maximum spreading diameter of impacting droplets on well prepared solid surfaces. Langmuir 21: 666-973.

Wakeman RJ, Tarleton ES (1992) Membrane characterisation: The need for a standard. Process Industry Journal: 16-19

List of Figures

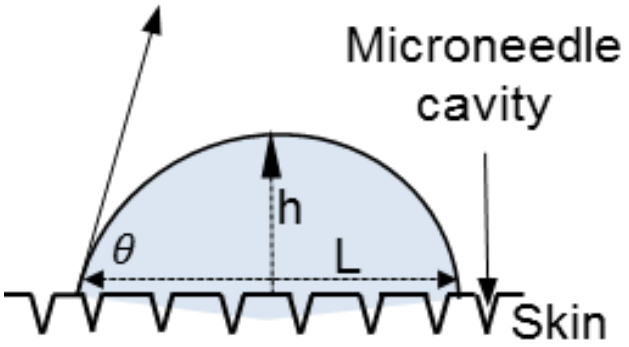

Figure 1. A liquid droplet on microneedle treated matrix and percolation of liquid into microcavities. The arrows illustrate droplet spreading radius (L), droplet height (h) and contact angle (θ).

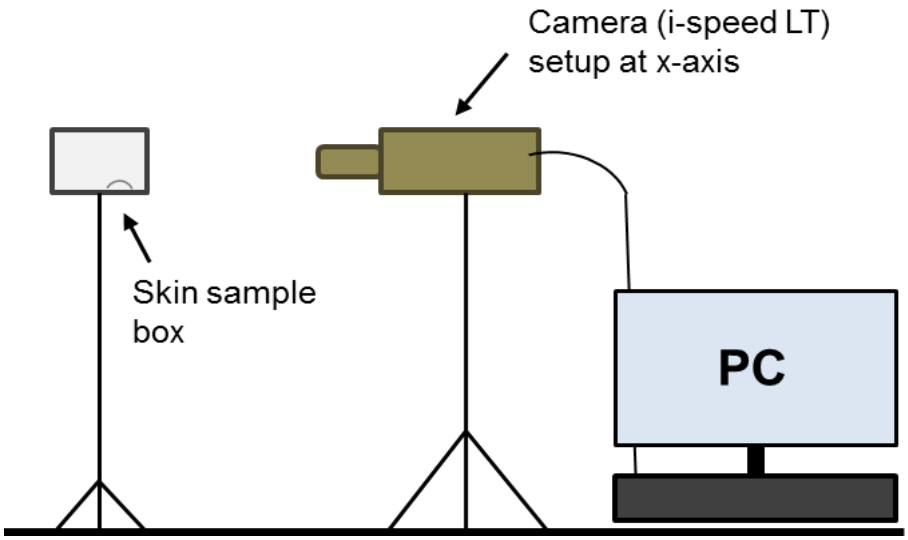

Figure 2. A schematic diagram of experimental setup for the capture of droplet spreading

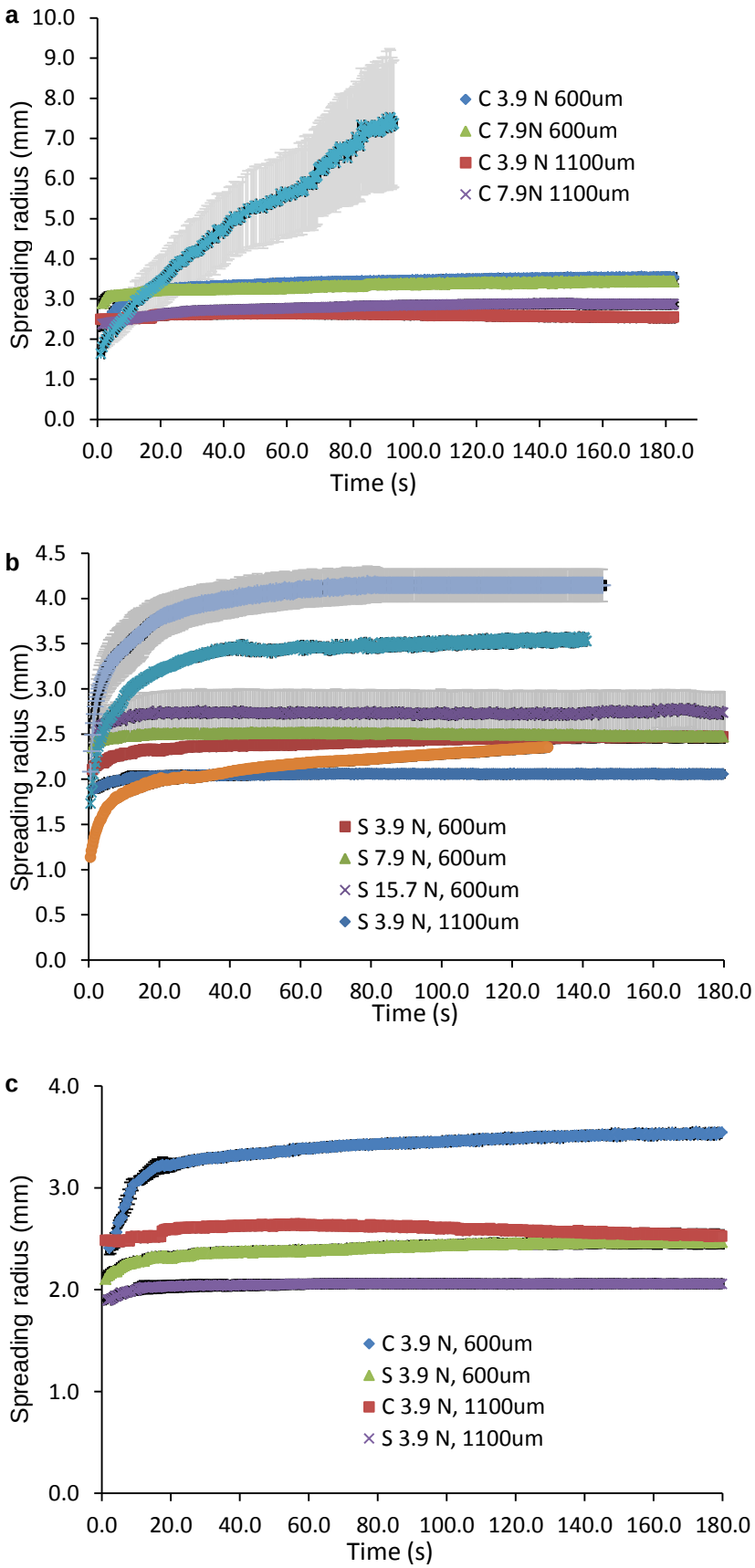

Figure 3. Time evolutions of droplet spreading radius for **a)** lidocaine solution on microneedle and non-microneedle treated skin **b)** lidocaine microgels on microneedle treated skin **c)** lidocaine solution and lidocaine microgels on microneedle treated skin. The abbreviation C is control lidocaine solution and S is sample lidocaine hydrogel.

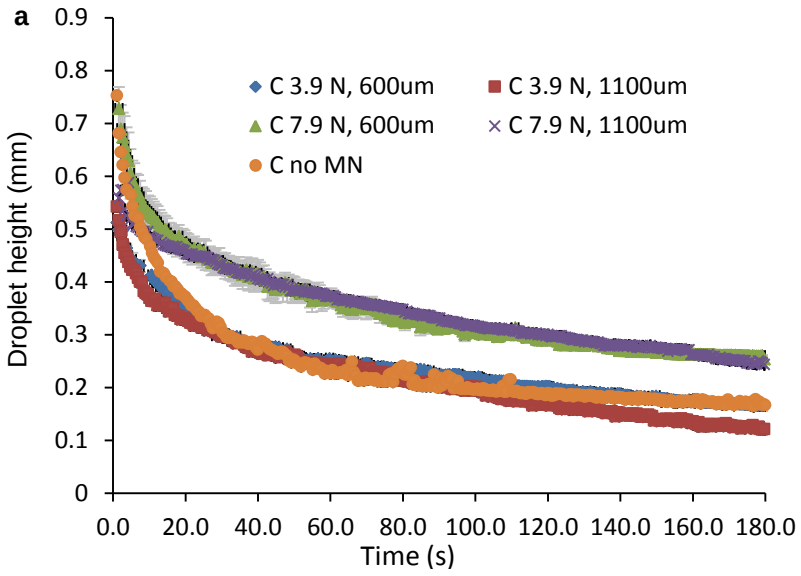
a
Droplet height (mm)
Time (s)
C 3.9 N, 600um
C 3.9 N, 1100um
C 7.9 N, 600um
C 7.9 N, 1100um
C no MN

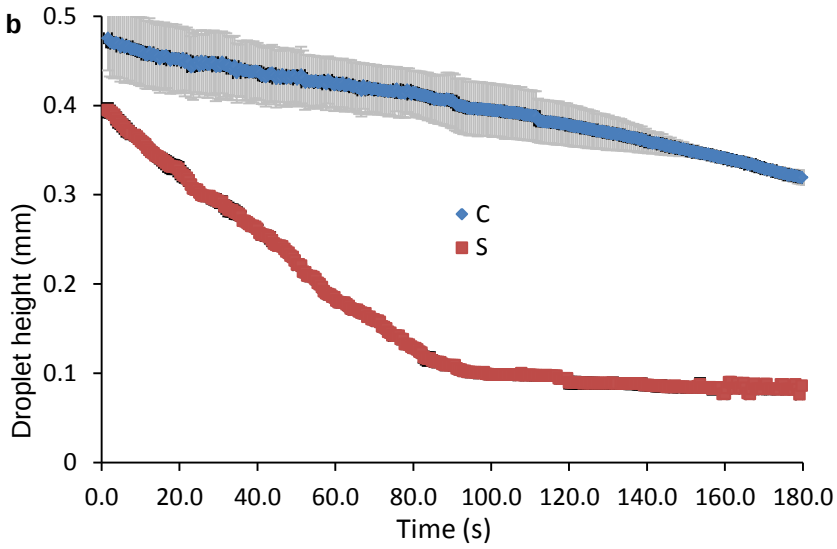
b
Droplet height (mm)
Time (s)
C
S

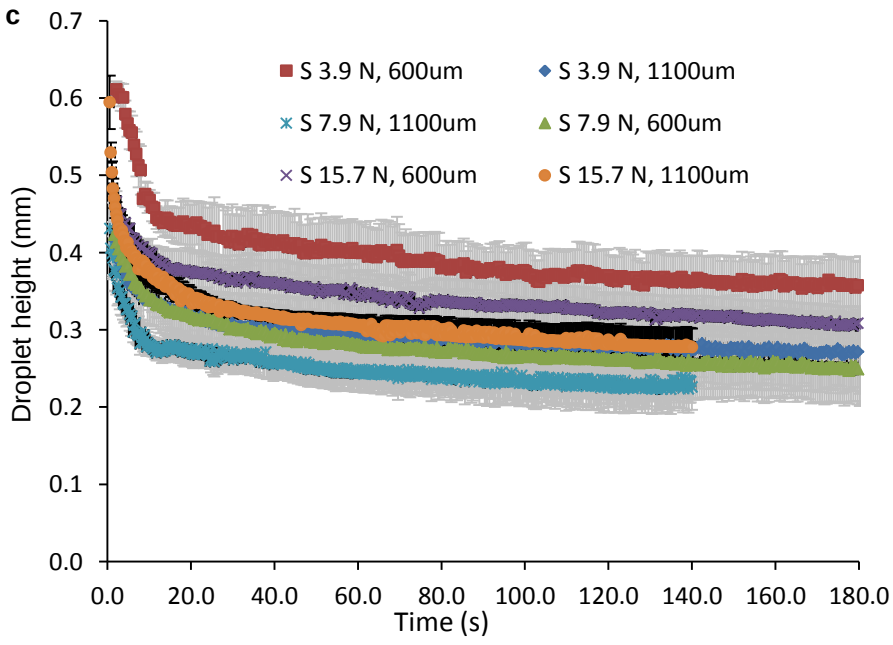
c
Droplet height (mm)
Time (s)
S 3.9 N, 600um
S 3.9 N, 1100um
S 7.9 N, 1100um
S 7.9 N, 600um
S 15.7 N, 600um
S 15.7 N, 1100um

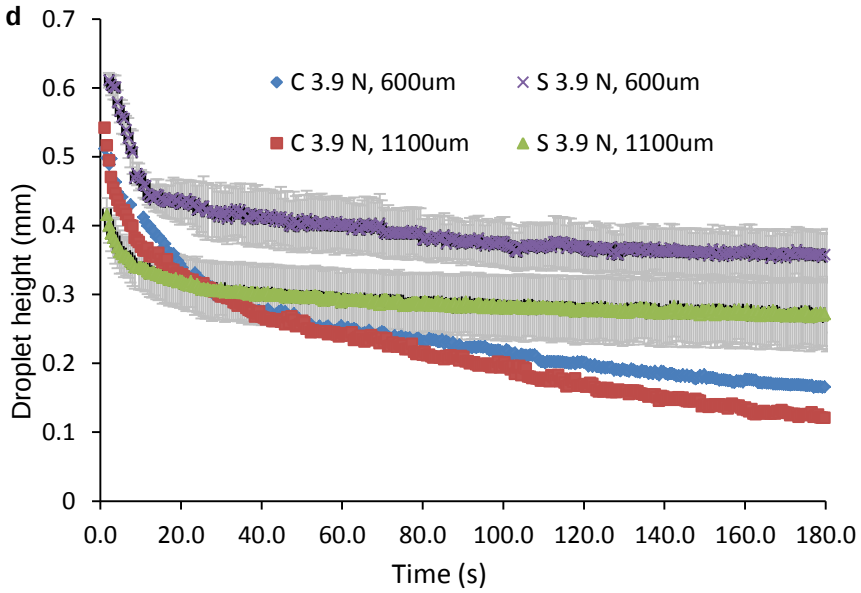

Figure 4. Time evolutions of droplet height for **a)** lidocaine solution on microneedle and non-microneedle treated skin **b)** lidocaine solution and lidocaine microgels on Strat-M membrane **c)** lidocaine microgels on microneedle and non-microneedle treated skin **d)** lidocaine solution and lidocaine microgels on microneedle treated skin. The abbreviation C is control lidocaine solution and S is sample lidocaine hydrogel.

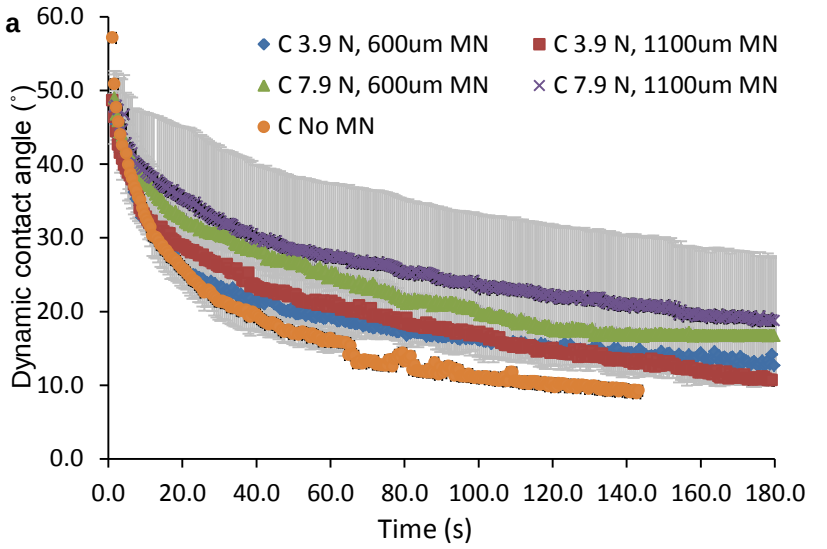
a
C 3.9 N, 600um MN
C 3.9 N, 1100um MN
C 7.9 N, 600um MN
C 7.9 N, 1100um MN
C No MN
Dynamic contact angle (°)
60.0
50.0
40.0
30.0
20.0
10.0
0.0
0.0 20.0 40.0 60.0 80.0 100.0 120.0 140.0 160.0 180.0
Time (s)

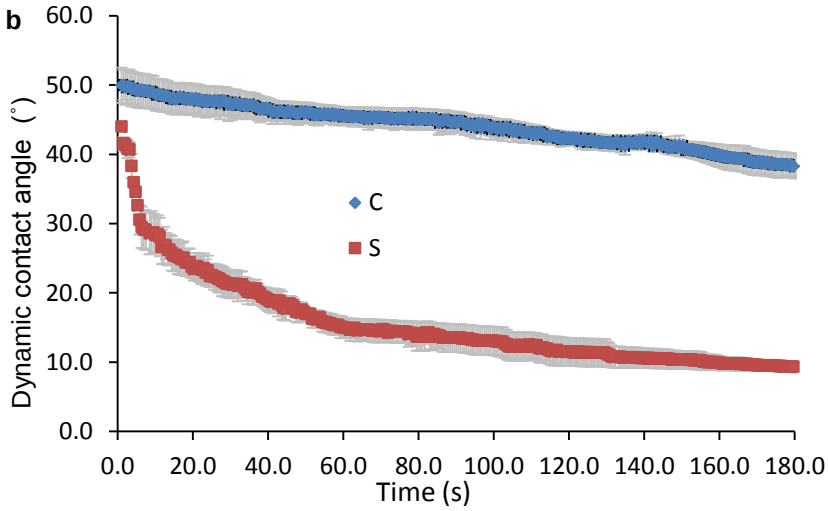
b
C
S
Dynamic contact angle (°)
60.0
50.0
40.0
30.0
20.0
10.0
0.0
0.0 20.0 40.0 60.0 80.0 100.0 120.0 140.0 160.0 180.0
Time (s)

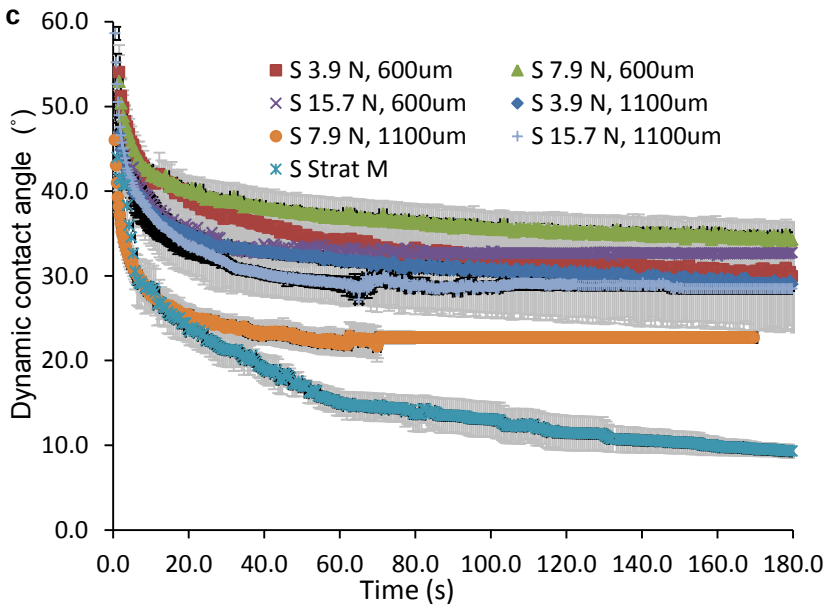
c
S 3.9 N, 600um
S 7.9 N, 600um
S 15.7 N, 600um
S 3.9 N, 1100um
S 7.9 N, 1100um
S 15.7 N, 1100um
S Strat M
Dynamic contact angle (°)
60.0
50.0
40.0
30.0
20.0
10.0
0.0
0.0 20.0 40.0 60.0 80.0 100.0 120.0 140.0 160.0 180.0
Time (s)

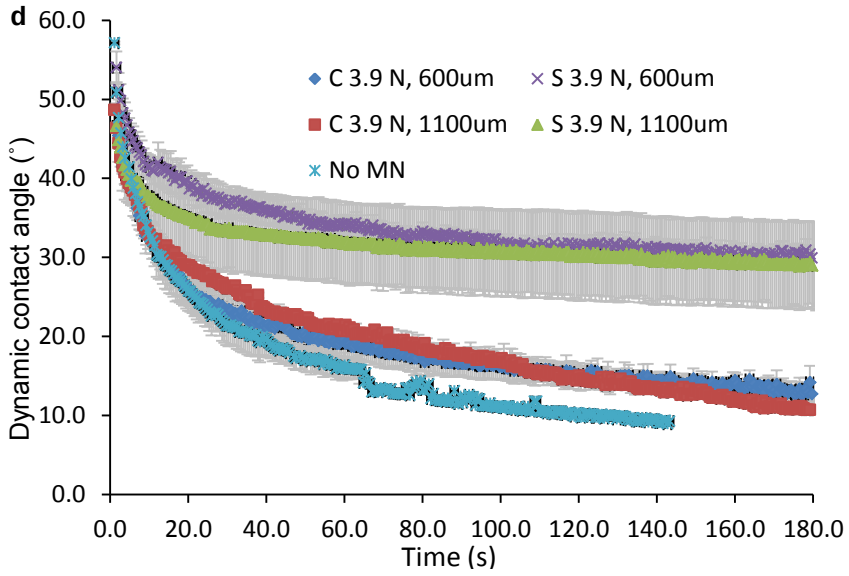

Figure 5. Time evolutions of dynamic contact angle for **a)** lidocaine solution on microneedle and non-microneedle treated skin **b)** lidocaine solution and lidocaine microgels on Strat-M membrane **c)** lidocaine microgels on microneedle and non-microneedle treated skin **d)** lidocaine solution and lidocaine microgels on microneedle treated skin. The abbreviation C is control lidocaine solution and S is sample lidocaine hydrogel.

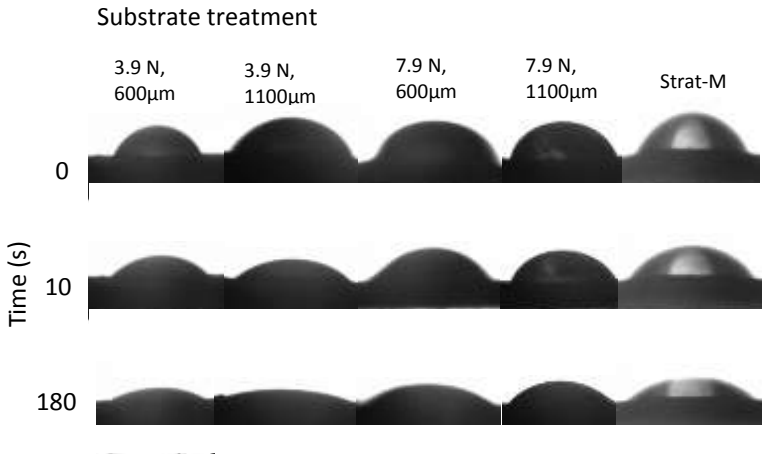

Figure 6. Captured images of lidocaine solution droplets (C) on a substrate (skin or membrane) at three different time points. The figure shows the droplet morphology at the substrate for different forces of MN insertion and MN lengths which were used to treat the skin.

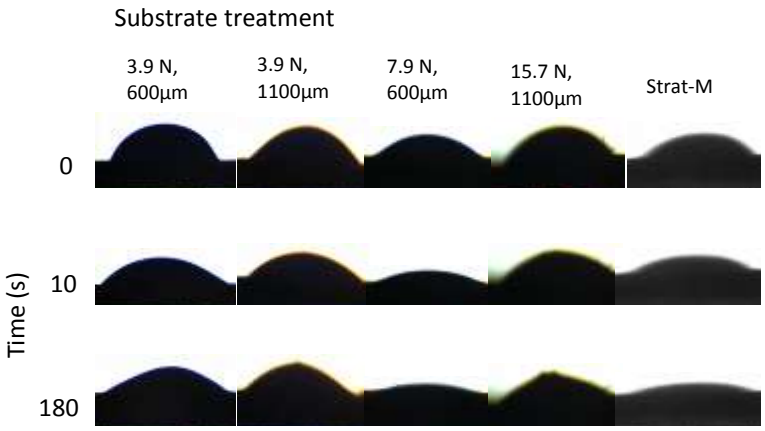

Figure 7. Captured images of lidocaine NaCMC:gel 1:2.3 hydrogel droplets (S) on a substrate (skin or membrane) at three different time points. The figure shows the droplet morphology at the substrate for different forces of MN insertion and MN lengths which were used to treat the skin.

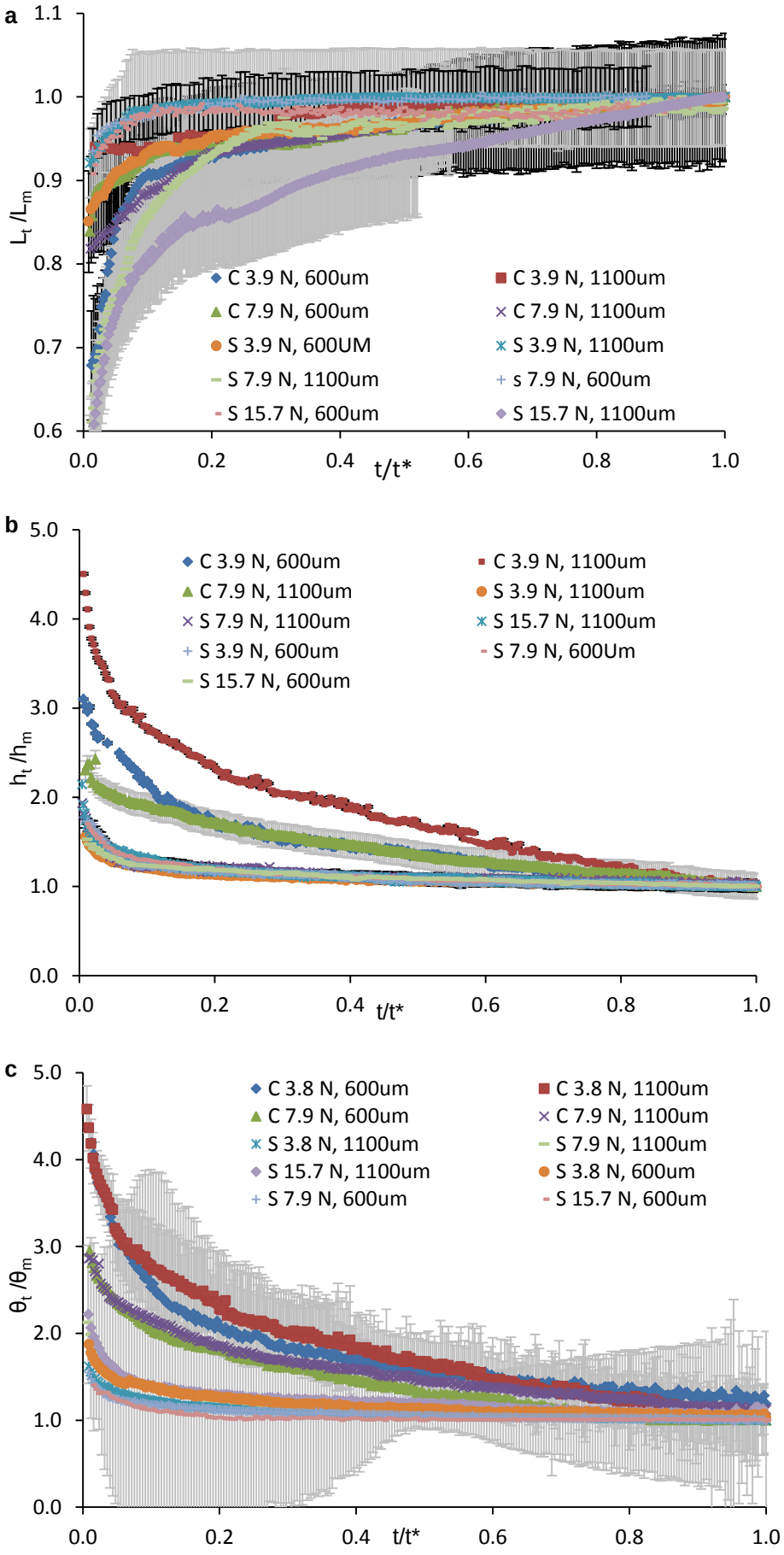

Figure 8. The lidocaine droplet plots outlining dynamic variation in **a)** spreading of hydrogel (S) or solution (C) on microneedle and non-microneedle treated skin **b)** droplet height of hydrogel (S) or solution (C) on microneedle and non-microneedle treated skin **c)** contact angle of hydrogel (S) or solution (C) on microneedle and non-microneedle treated skin.

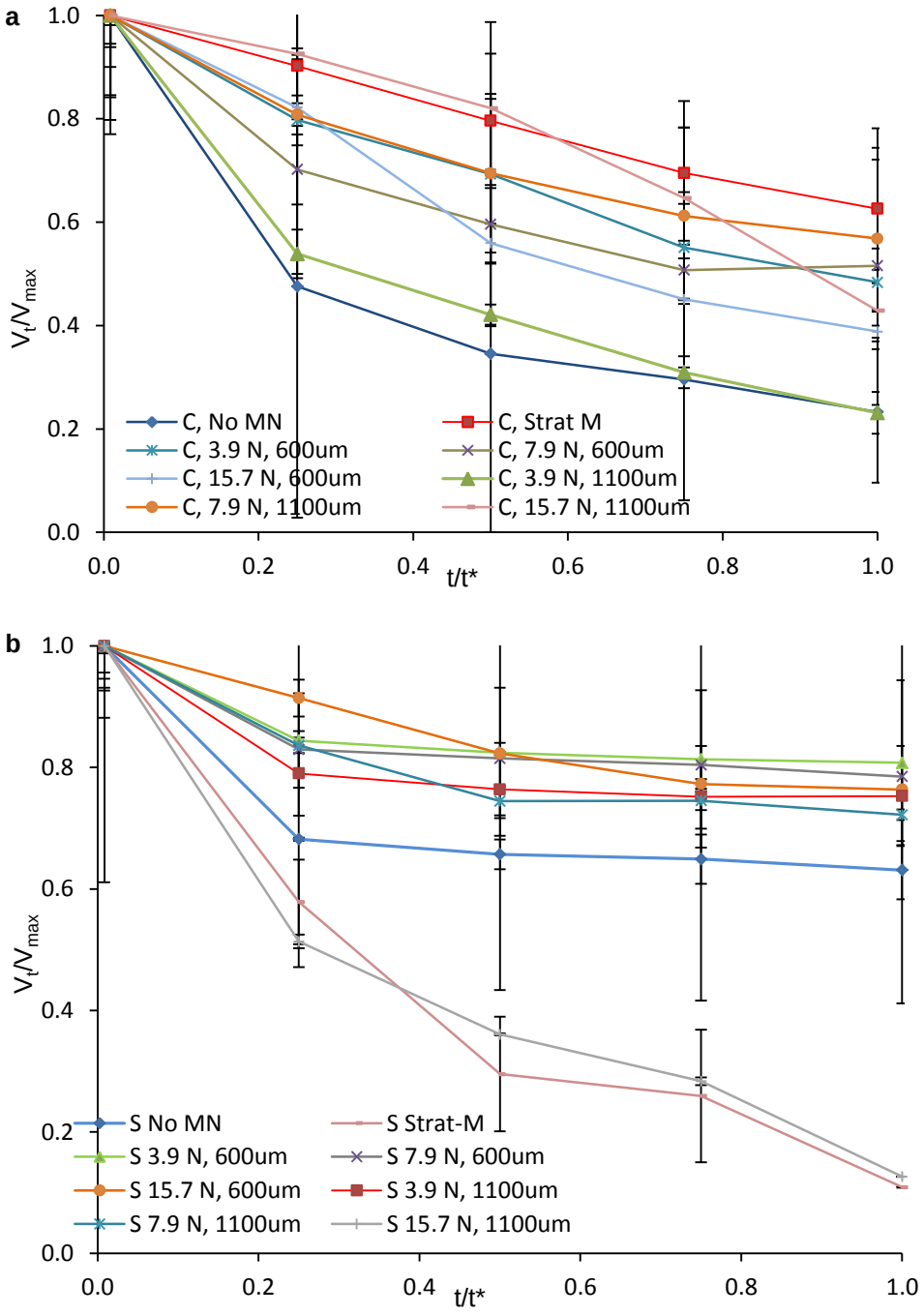

Figure 9 The non-dimensional droplet volume on top of skin sample **a)** for lidocaine solution **b)** lidocaine NaCMC:gel 1:2.3. The abbreviation C is control lidocaine solution and S is sample lidocaine hydrogel.